https://erjm.journals.ekb.eg
ISSN: 1110-1180

DOI: ---------

ERJ
Engineering Research Journal
Faculty of Engineering
Menoufia University

Numerical Investigation on the Performance of Vortex Tube

Esmail.A.Koraim[1]*, Sobieh Selim[2], A.A Abdel-Hamied [2], A.A. Hussien [2]

[1] Mechanical Department, Faculty of Engineering, Sinai University, North sinai, Egypt.*
[2] Mechanical Power Department, Faculty of Engineering, Menoufia University, Menoufia, Egypt.
(Corresponding author: as_amien@sh-eng.menofia.edu.eg)

ABSTRACT
The current study presents numerical investigation of the vortex tube performance. ANSYS-15 software and its' tools are used to simulate the flow through vortex tube. The basic governing equations of mass, momentum and energy conservation in addition turbulence equations are used to predict the flow along vortex tube. 3-D, compressible and turbulent flow with certain boundary conditions are applied to calculate the flow parameters. Comparisons between published experimental data and present numerical results are performed to select the suitable turbulence model and to valid the numerical model. The validation appeared that standard *(k-ε)* is the best turbulence model based on the calculated coefficient of correlation. The effect of operating conditions (inlet pressure, cold mass fraction m_{cf} and geometric parameters of vortex tube such as number of inlet nozzles, hot tube length and diameter with constant ratio D_c/D_h on vortex tube performance are studied. The numerical results show that, the maximum values of cooling and heating coefficient of performance is achieved at lowering inlet pressure. The hot and cold temperature differences increase with increasing inlet pressure. The maximum cold temperature difference can be obtained at m_{cf} between 0.22 and 0.36 when the inlet pressure changes from 1.0 to 5.0 bar. The hot temperature difference increases with increasing m_{cf} for all studied inlet pressures. The numerical results indicated that the highest value of cold and hot temperature differences achieved at hot tube diameter, hot tube length (L_h) and diameter ratio D_c/D_h of 1.3 cm, 25 cm and 0.5 respectively.

Keywords: *Vortex tube; Numerical simulation; Operating inlet pressure; Energy separation; Coefficient of performance.*

1. Introduction

The vortex tube is a thermal-mechanical device that allows compressed air to be separated into cold stream and hot stream. The vortex tube consists of one or more inlet nozzles, vortex chamber, a cold tube, hot tube, and hot end control valve (cone valve). The operation theory of vortex tube is depended on injecting compressed air into the vortex chamber via the one or more nozzle slots and then energy separation mechanism occurs. Figure (1) shows the vortex tube and its components and the air streams. The tangential injection of compressed air expands and creates strong rotating layers of air inside the vortex tube. Based on the air vortex motion and radial pressure distribution, two streams are formed. The hot air stream is around the circumference of the main tube and exit from around the control valve, while the cold air stream in the tube center is collided with the control valve and flows in the opposite direction of the hot stream to exit from the cold tube. Separated cold or hot streams, can be employed according to the industrial requirements. Based on the direction of hot and cold streams, the vortex tube can be classified into counter-flow and parallel flow vortex tube [1]. Many studies are attempted to investigate the performance of vortex tube. Comparison between the suitability of turbulence models to predict the temperature difference in a vortex tube was studied by [2].

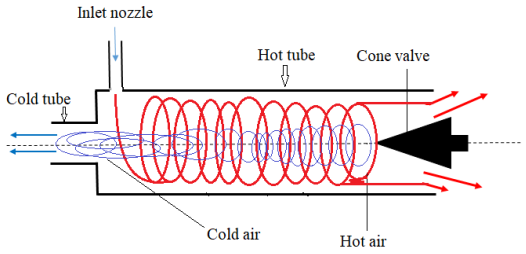

Figure (1): The components and operation theory of vortex tube.

The results indicated that, standard $(k-\varepsilon)$ is the more suitable for predicting the temperature distribution along the vortex tube. 3-D computational model to study the effect of the number of inlet nozzle on the flow and cooling power consumption of the vortex tube was presented by [3]. Inlet nozzles numbers (N = 2, 3, 4, 6, and 8 nozzles) were created and modeled by employing standard $(k-\varepsilon)$ turbulent model. The results indicated that the increased number of inlet

nozzles increases the cooling capacity substantially while the cold outlet temperature decreases moderately. The computational fluid dynamic (CFD) model was created by [4], based on a commercial vortex tube. A two-dimensional (2D) model with standard ($k-\varepsilon$) and renormalization group RNG ($k-\varepsilon$) turbulence models were used to simulate flow through vortex tubes. The comparison between theoretical results and experimental data showed that, the two-turbulence model (standard ($k-\varepsilon$) and renormalization group RNG ($k-\varepsilon$)) is achieved convergence to predict the numerical results. The computational analysis of flow feature and energy separation in a vortex tube with a different number of inlet nozzles (1, 2, 3, 4, 5, and 6 nozzles) and air working fluid presented by [5]. The results presented that the kinetic energy decreased with the increased number of nozzles. At the same time, the highest temperature difference occurred at an odd number of inlet nozzles. The effect of different inlet shapes (pipe and nozzle) on the performance of vortex tubes was studied experimentally by [6]. They concluded that the inlet nozzle shape gives the best performance. The effect of number of inlet nozzles (2, 3, and 6 nozzles) on the cooling performance of vortex tubes was studied by [7]. The experimental results showed that 3 inlet nozzles give the best cooling performance. The effect of inlet nozzles number (2, 4, and 6 nozzles) on cold temperature difference and performance of vortex tube was presented by [8]. They concluded that 2 inlet nozzles give the maximum temperature difference and performance. The effect of inlet nozzles number (2, 3, 4, 5, and 6) with different nozzle materials (fiberglass, aluminum, and steel) on performance of vortex tube was shown by [9]. The results, presented that the best performance was achieved at 6 nozzles number with steel material in a vortex tube. The effect of the number of different nozzles with test gases such as oxygen and air on the temperature drop was studied by [10]. They found that oxygen achieve the best temperature drop compared with air at all number of inlet nozzles. The number of nozzles (1, 2, and 4 nozzles) and cold tube diameter on the temperature difference tested by [11]. They found that the 4 nozzles and D_c=0.5 D_h achieve the higher temperature difference. The effect of the valve angle of counterflow vortex tubes on thermal energy separation in a vortex tube was investigated by [12]. They discovered that the valve angle had little impact on system performance. conducted experiments with various conical valve angles and discovered that the maximum temperature difference occurred at valve angles of 30° or 60° [13]. **T**he impact of different valve angles (30°,45°,60°,75°, and 90°) on the vortex tubes performance was investigated by [14]. The results showed that valve angles of 45° offer the highest cooling effect while valve angles of 60° provide the optimum heating effect. An experimental study conducted by [15]. They studied the effect of cold tube diameter (5, 6, and 7mm) on the performance of vortex tubes. The results presented that, the cold tube diameter at 6 mm gives the best performance. Experimentally, studied the effect of cold tube diameters and inlet pressure at (4, 5, 6, and 7 bar) on the temperature difference of vortex tube by [16]. The results indicated that, the increase in cold tube diameter increased the hot temperature difference and at the same time decreased the cold temperature difference. The performance of the vortex tube investigated by [17] under various design parameters such as inlet air pressure, length and diameter of hot tube. The testing results revealed that higher inlet air pressure levels resulted in a maximum temperature difference with lowering COP . Also, the optimum length of hot tube is between 66 mm to 158 mm and the optimum hot tube diameter 9 mm to 26 mm. The effect of length to diameter ratio (L_h/D_h) on the temperature difference of vortex tube was investigated experimentally by [18]. the result reported that the maximum temperature difference of vortex tube achieved between the range ($20 \leq L_h/D_h \leq 55$). The effect of hot tube divergent on vortex tube performance under boundary and geometry conditions diameter ratio (cold tube diameter/ hot tube diameter) 0.5, valve angle 45°, number of inlet nozzles 6, angle of hot tube divergent 3°, and cold mass fraction from 0 to 1 was investigated by [19]. The results presented that the maximum-cold temperature occurs at a cold mass fraction 0.23 but, the maximum-hot temperature is achieved at a cold mass fraction 0.4. Additionally, concluded that the COP decreased with an increase the inlet pressure. The effect of different design parameters on the vortex tube performance was studied by [20]. They concluded that the maximum performance of vortex tube is achieved at length and diameter of hot tube 194 mm, 14.6 mm respectively, 4-inlet nozzles, and nozzle diameter of 1.8 mm. Additionally, the results showed that the cold and hot temperature difference increase with increased inlet pressure. In spite of existing extensively research sources about vortex tube, understanding of its energy separation mechanism know-how needs some thinkable investigations yet.

In this way, the present paper aims to study numerically the effects of operating conditions and geometrical parameters such as inlet pressure, cold mass fraction, diameters and lengths of hot tubes and numbers of inlet nozzles to attain reasonable performance. The obtained results will be discussed to select the suitable operating conditions and

geometrical parameters that achieved the best performance of vortex tube.

2. Numerical Simulation

CFD technique based on the basic governing equations plays a powerful alternative to simulate and predict airflows in vortex tubes. ANSYS-15 software is used to perform numerical modeling of the vortex tube.

2.1 Governing equations

The numerical simulation of the flow through the vortex tube was carried out using the Fluent CFD code system. In this study, the flow is assumed as steady, turbulent, compressible and perfect gas. For 3-D flow, conservation of mass, momentum, and energy equations are used to simulate the flow through the vortex tube. The governing equations can be written as the follows, [21]:

- The mass conservation equation (The continuity equation)

$$\nabla \cdot (\rho \vec{v}) = 0 \qquad (1)$$

- The momentum conservation equation

$$\nabla \cdot (\rho \vec{v}\vec{v}) = -\nabla P + \nabla \cdot (\bar{\bar{\tau}}) + \rho \vec{g} \qquad (2)$$

- The energy conservation equation

$$\nabla \cdot \left(\vec{v}(\rho E + P)\right) = \nabla \cdot \left(\kappa_{eff} \nabla T\right) + \nabla \cdot (\bar{\bar{\tau}} \cdot \vec{v}) \qquad (3)$$

where the E is the total energy, κ_eff is the effective thermal conductivity

$$\kappa_{eff} = k + C_p \mu_t / Pr_t \qquad (4)$$

Based on the compressible flow the main properties of air (ideal gas) can be calculated from the state equation:

$$P = \rho RT \qquad (5)$$

2.2 Turbulence model

The standard k-ε turbulence model is used in the present simulation for describing the turbulent flow behavior inside vortex tube. The transport equations are given as:

- Turbulent Kinetic energy (k) equation

$$\nabla \cdot (\rho \vec{v} k) = \nabla \cdot \left[\left(\mu + \frac{\mu_t}{\sigma_k}\right) \nabla k\right] + G_k + G_b - \rho\varepsilon - Y_m + s_k \qquad (6)$$

- Dissipation rate (ε) equation

$$\nabla \cdot (\rho \vec{v} \varepsilon) = \nabla \cdot \left[\left(\mu + \frac{\mu_t}{\sigma_\varepsilon}\right) \nabla \varepsilon\right] + C_{\varepsilon 1} \frac{\varepsilon}{k} (G_\varepsilon + G_{\varepsilon 3} G_b) - C_{\varepsilon 2} \rho \frac{\varepsilon}{k} + S_\varepsilon \qquad (7)$$

The turbulent viscosity, μ_t, is computed by combining k and e such that:

$$\mu_t = \rho \, C_\mu \, k^2 / \varepsilon \qquad (8)$$

Y_m, represents the contribution of the fluctuating in compressible turbulence to the overall dissipation rate and turbulence model constants of standard k-ε are $c_{\varepsilon 1} = 1.44, c_{\varepsilon 2} = 1.92, \; c_\varepsilon = 0.09, and \; Pr_t = 0.85.$

2.3 Computational Domain and Grid generation

The configuration of tested vortex tube is defined on ICEM-CFD software. Grid is engineered by ICEM software. During this study patch confirming algorithm by tetrahedrons method is used to generate the meshed size for all edges [22]. Figure (2) represents the computational domain for the studies vortex tube geometry after creating the grid and intense the number of cells at inlet nozzle, cold outlet and hot outlet. The geometrical details of the tested vortex tube are given in Table (1).

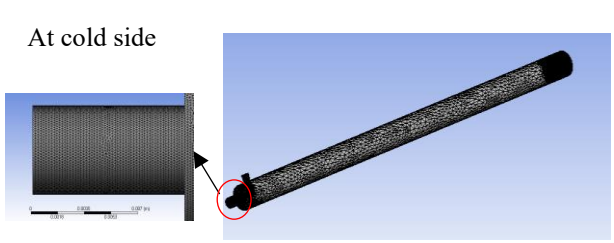

Figure (2): Meshing domain of vortex tube with one nozzle.

Table (1) Geometrical details of studied vortex tube.

Geometrical Parameter	*Value*
Length of hot tube (L_h)	cm, 50 cm, and 75 cm 25
Diameter of hot tube (D_h)	cm, 1.3 cm, and 1.95 0.65 cm
Length of cold tube (L_c)	cm 1
Diameter ratio of cold to hot tube (D_c/ D_h)	0.5
Number of inlet nozzles (N)	and 4 ,3 ,2 ,1
Diameter's ratio of nozzle	0.5
Cone valve angle	°45

The cold and hot temperature difference of vortex tube can be used to select and judge the sufficient cell number, [22]. The effect of different cells number on

the cold/hot temperature difference at one inlet nozzle, 5.0 bar pressure inlet and 50 cm length of hot tube is shown in table (2). From the table, it can be observed that, increasing of cells number increased the difference of temperature to reach the cells numbers (289745). Afterwards no much benefit is observed with increasing the number of cells with respect to the required time and CFD capacity of solution.

Table (2) Test different grid numbers of vortex tube at 1 nozzle and P_i=5bar.

Cells .No	*156963*	*201457*	*251807*	*289745*	*321216*
ΔT_c	*4.45*	*5*	*5.78*	*5.81*	*5.82*
ΔT_h	*5*	*5.5*	*6.07*	*6.09*	*6.1*
m_c (kg/s)	*0.0055*	*0.00579*	*0.00581*	*0.00582*	*0.00584*
m_h (kg/s)	*0.0115*	*0.0113*	*0.0112*	*0.011*	*0.0108*

2.4 Boundary conditions

The numerical solution for CFD model depends on applying accurate boundary conditions. These conditions are integrated within the numerical model. During this study, there are three types of boundary conditions, namely inlet, outlet, and wall boundary conditions. The inlet conditions are set as pressure inlet which is normal direction on nozzle entry. The value of inlet pressure is defined as gauge total pressure and its value will change between 1.0 bar to 5.0 bar according to operating conditions. The outlet conditions of hot and cold flow are assumed as pressure outlet and its value is equal to zero-gauge pressure. In addition, a no-slip velocity boundary conditions are applied of all walls of the studied vortex tube and simultaneously they are assumed to be adiabatic. At the same time, the initial condition of turbulence is selected as turbulence intensity with 5% and turbulence viscosity ratio is 10. Figure (3) shows the applied boundary conditions of vortex tube domain.

2.5 Solution scheme

The flow chart of the CFD model solution is shown in figure (4). The pressure-based, steady-state solver with the standard *k-ε* turbulent model is taken for the analysis with standard wall functions. The simple scheme is used for energy equations. The convergence limitations for the residuals regarding mass, momentum and energy equations are set on 10^{-5}

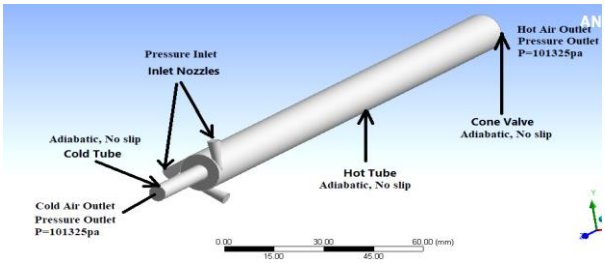

Figure (3): Boundary conditions in a vortex tube.

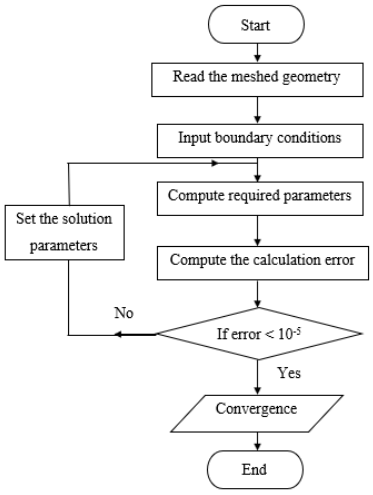

Figure (4): The flow chart of CFD Solution.

Based on the changing of the temperature gradient and air velocities along the vortex tube, some parameters are calculated to describe the vortex tube performance. These parameters include the cold and hot temperature differences, cold mass fraction (m_{cf}) and coefficient of performance (*COP*) of the vortex tube. The following equations are used to calculate cold and hot temperature difference:

$$\Delta T_c = T_i - T_c \quad (9)$$

$$\Delta T_h = T_h - T_i \quad (10)$$

$$m_{cf} = \frac{m_c}{m_i} \quad (11)$$

The coefficient of performance (*COP*) of vortex tubes is calculated based on the propose of vortex tube (cooling or heating). COP can be defined as the ratio of the cooling/heating load to the isothermal compression energy [17, 23] as the following equations:

$$COP_c = \frac{\gamma}{\gamma - 1} m_{cf} \frac{(T_i - T_c)}{T_i ln\left(\frac{P_i}{P_a}\right)} \quad (12)$$

$$COP_h = \frac{\gamma}{\gamma-1}(1 - \dot{m}_{cf})\frac{(T_h - T_i)}{T_i ln\left(\frac{P_i}{P_a}\right)} \quad (13)$$

3. Mathematical Model Validation

To validate the mathematical model, a comparison between the present numerical results using standard $(k-\varepsilon)$ model with the published experimental data is performed. Two different cases are used as test cases to perform a comprehensive validation of the theoretical model. The first validation case is conducted with using [14] by creating the geometry on ICEM software then it is reading by Fluent-ANSYS with the same dimensions and the same operating and boundary conditions. The present model is used to simulate and predict the flow along their geometry. The comparison of the experimental data reported by [14] and the present theoretical results is performed. The theoretical study is performed with using the cone valve angles of 30°, 45°, and 60° and the results are shown in figure (6). This figure indicated that the predicted results from the CFD model of cold/hot temperatures and cooling performance are acceptable to some extent with the published experimental data for all inlet pressures at different cone valve angles. Another validation includes a comparison between the experimental data reported by [16] and the theoretical results of the present CFD model. Figure (6) depicts a comparison of theoretical results with experimental data [16] at different cold tube diameter (D_c = 6 and 7 mm). From this figure, it can be observed that there is considerable qualitive agreement between the present theoretical results and published experimental data for all values of the cold tube diameter. From the previous comparisons, it can be concluded that the current CFD model (ANSYS software) can be predict the flow properties of air along the vortex tube with an acceptable accuracy.

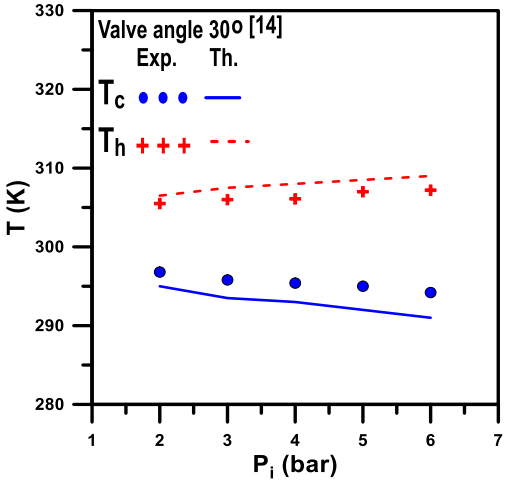

Fig. (5-a)

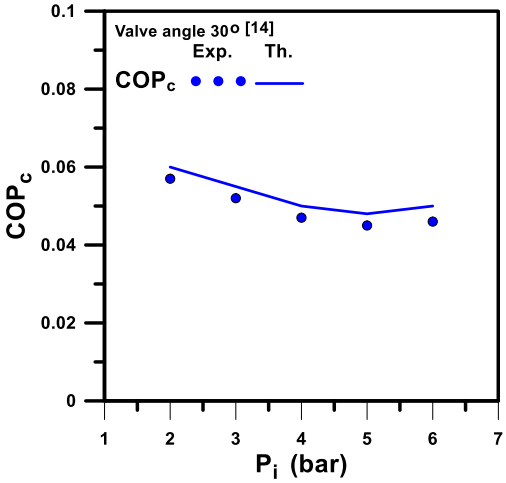

Fig. (5-b)

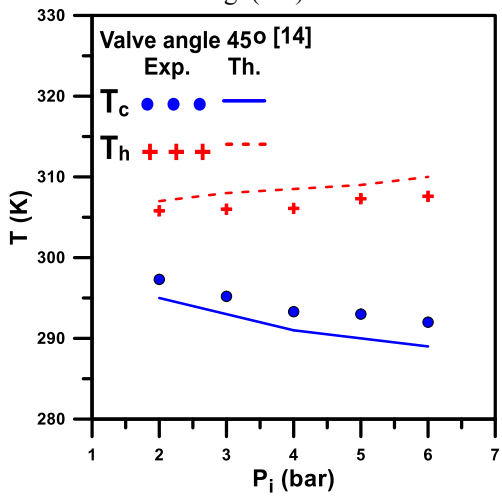

Fig. (5-c)

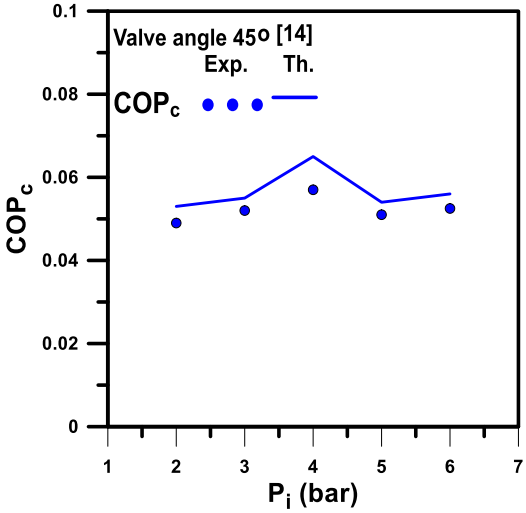

Fig. (5-d)

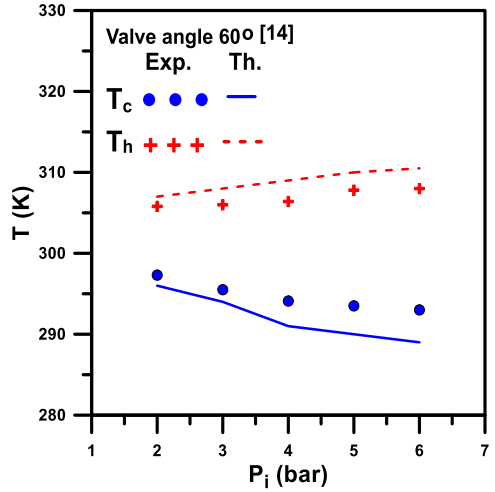

Fig. (5-e)

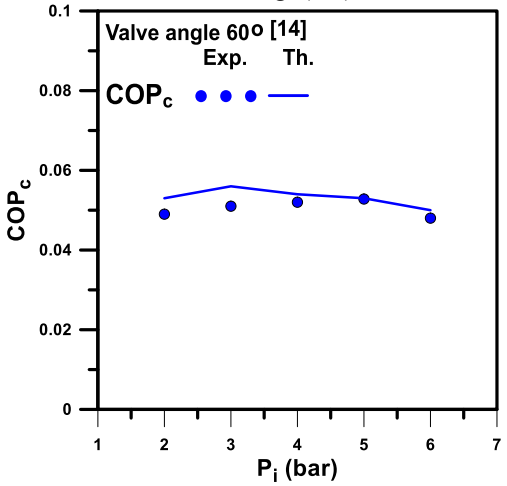

Fig. (5-f)

Figure (5): Comparison between published experimental data [14] and numerical results of the cold /hot exit temperature and cooling coefficient of performance at different values of cone angles.

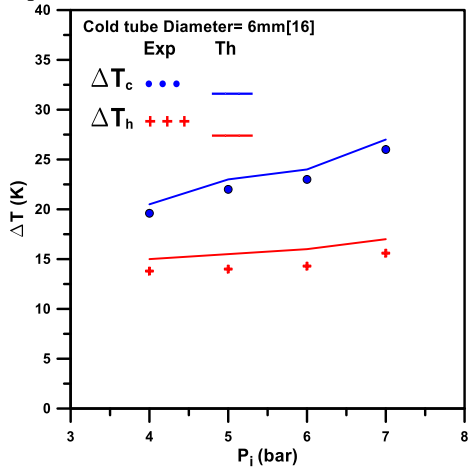

Fig. (6-a)

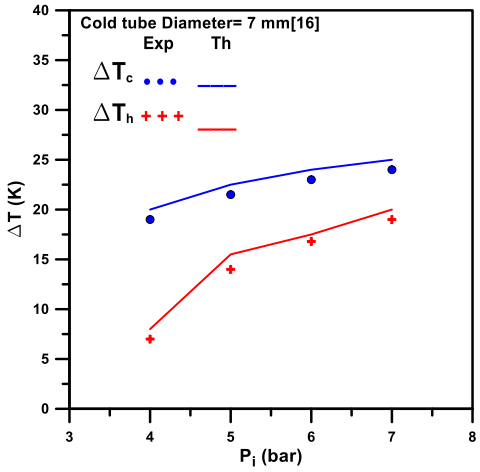

Fig. (6-b)

Figure (6): Comparison of cold temperature difference with inlet pressure at cold tube diameters 6 mm and 7 mm [16].

From the literature review about predicting temperature and flow during vortex tube observed that, the suitable turbulence model recommended is not fixed. Some studies concluded that standard $(k-\varepsilon)$ model [2, 3] is valid and other researches recommended with RNG $(k-\varepsilon)$ model [4]. On the other hand, some studies presented realizable $(k-\varepsilon)$ model [21] is more suitable for predicting the temperature distribution inside vortex tube. To determine and select the more suitable turbulence model during the present study, three turbulence models (standard $k-\varepsilon$, RNG $k-\varepsilon$ and realizable $k-\varepsilon$) are applied and compared with previous published data [14]. The comparison between results .is presented in Fig. (7)

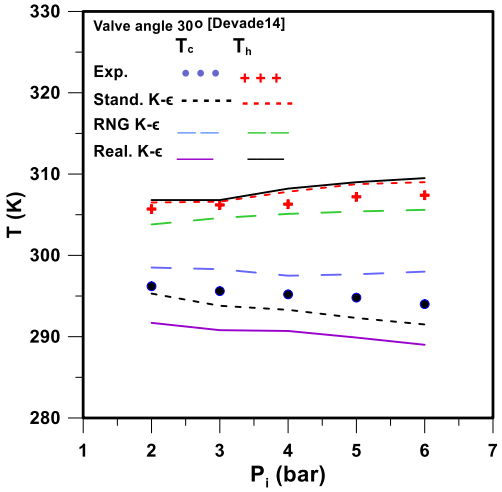

Figure(7): Comparison between published experimental data and numerical results of different turbulence models for the cold /hot exit temperature.

From the figure, it can be observed that the predicted results of tested turbulence model are acceptable values. To judge the more suitable turbulence model, coefficient of correlation (R^2) is estimated of all turbulence models as follow:

$$R^2 = 1 - \frac{Difference\ between\ measured\ and\ predicted\ parameters}{Experiental\ results\ deviation}$$

$$R^2 = 1 - \frac{\Sigma(\emptyset_{Exp} - \emptyset_{pred})^2}{\Sigma(\emptyset_{Exp} - \emptyset^-_{Exp})^2} \qquad (14)$$

where ϕ_{Exp} is the experimental value of flow parameter at a certain point in the domain and ϕ_{Pred} is the predicted value of the same flow parameter at the same point. The term $\emptyset^-_{Exp}$ in the last equation is defined as:

$$\emptyset^-_{Exp} = \frac{\sum_{i=1}^{n} \emptyset_{Exp}}{n} \qquad (15)$$

Where *n* is the number of experimental points. Based on the theoretical and experimental results, R^2 is calculated of each turbulence model and presented in table (3).

Table (3): The Coefficient of correlation (R^2) of turbulence models.

Turbulence model	*Coefficient of correlation (R^2)*	
	T_c	T_h
$(k-\varepsilon)$ *standard*	*0.9964*	*0.9985*
RNG $(k-\varepsilon)$	*0.9896*	*0.9879*
Realizable $(k-\varepsilon)$	*0.9752*	*0.9975*

The high value of the correlation coefficient means that the numerical results are more accurate. Therefore, from table (3) it can be noticed that the standard $(k-\varepsilon)$ gives a higher value of (R^2) at a cold and hot temperature and this is consistent with [2]. So, it will be used to obtain the theoretical results during the present study.

4. Numerical Results and Discussion

The numerical results of the suggested geometry of vortex tube based on the simulation of a 3-D model with standard $(k-\varepsilon)$ turbulence model will be displayed and discussed on the next section. The theoretical study is conducted to simulate and calculate the flow properties.

4.1 The flow characteristics and the swirling effect

The suggested geometry of vortex tube with two inlet nozzles and 25 cm hot tube length is simulated to describe the flow characteristics and swirling effect. The velocity and temperature distributions at four positions along the hot tube of vortex tube are shown in Fig. (8). The tangential velocity component at different positions along hot tube length is shown in Fig. (8-a). From the figure, it can be noticed that the higher tangential velocity is achieved at cross sectional near to the inlet of the vortex tube (z/L_h=0.05). With far away from inlet of vortex tube the value of tangential velocity component is decreased as shown at z/L_h=0.25, at z/L_h=0.50 and at z/L_h=0.75 respectively. At the same time, the flow direction of hot stream (at outer radius) and the cold stream (at the tube center) is changed based on the cold and hot mass flow rate as shown in Fig (8-b). at the tube center, the cold flow has the higher axial velocity with near from the inlet nozzle and it decreases with towards of hot outlet. Based on the vortex effect and energy separation of vortex tube, the tangential intensity is decreased along the tube radius and tube length. Figure (8-c) shows the color vector velocity of the tangential velocity component. To display the effect of swirling motion on the flow properties along the vortex tube, the swirling number is used to determine change of swirl strength along the hot tube length.

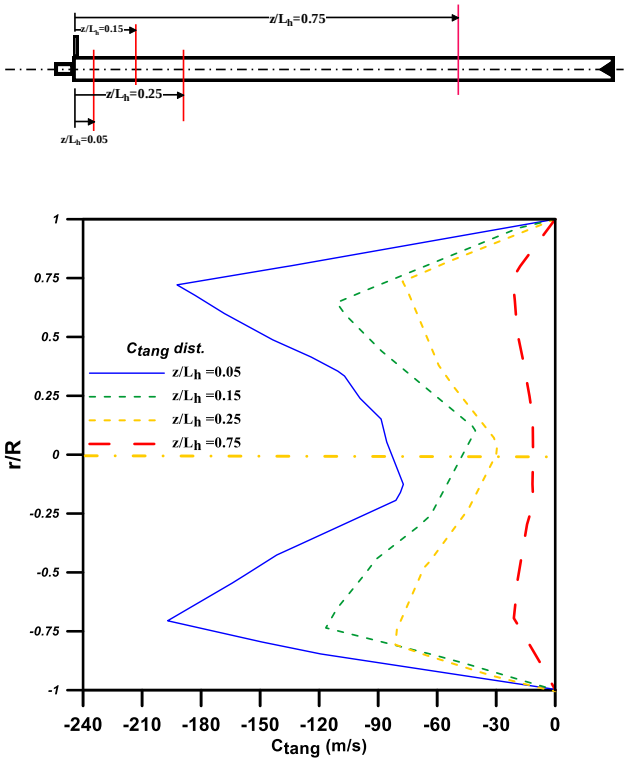

Fig. (8-a)

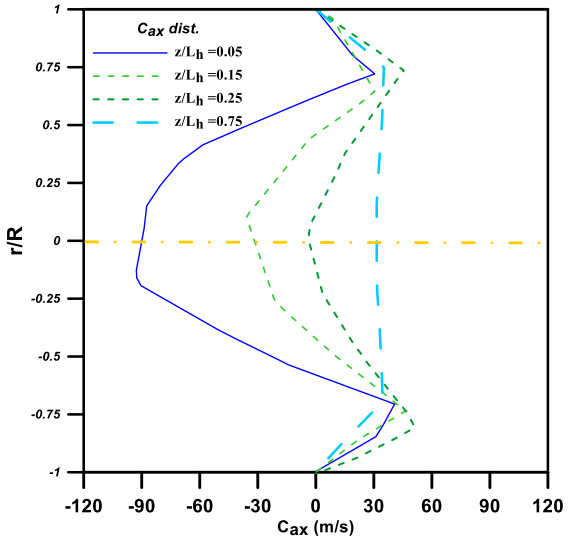

Fig. (8-b)

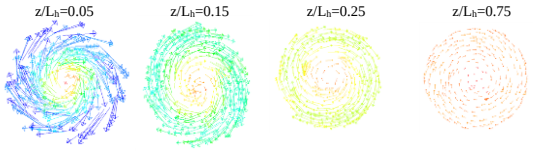

Fig. (8-c)

Figure (8) the velocity distribution along the hot tube length.

The swirl number, S, is defined as, the ratio of swirl momentum $G_{\emptyset}$, to the axial flux linear momentum G_x ,and it is defined as [24]

$$S = \frac{G_{\emptyset}}{R\,G_x} = \frac{\int_0^R C_{ax} C_{tang} r^2 dr}{R \int_0^R C_{ax}^2 r dr} \qquad (16)$$

Where R, is the radius of tube. In general, the strength of swirl can be categorized as either weak swirl (S < 0.6) or strong swirl (S > 0.6), [24]. Figure (9) presents the swirl number of four tested positions of vortex tube at different values of inlet pressure. From the figure, it can be concluded that the swirl number is higher at the positions near the inlet of vortex tube and is smaller near the hot exit for all inlet pressure values. Also, the reduction of inlet pressure tends to decrease in the swirl number at all positions and the maximum swirl number occurred at z/L$_h$=0.05 while the minimum swirl number occurred at z/L$_h$=0.75. The decay of swirl is accelerated with the increase of the inlet pressure of compressed air.

The high values of tangential and axial velocity distribution reflected on the pressure and temperature gradient along the vortex tube (energy separation). This effect is cleared on the results of total temperature distribution along the radial and axial directions of hot tube length. The change of the total temperature along the tube radius at different positions (z/L$_h$ =0.05, 0.15, 0.5 and 0.75) is shown in Fig (10-a).

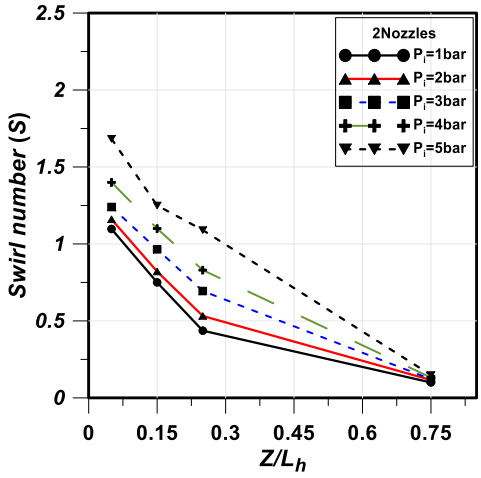

Figure (9): Effect of inlet pressure on decay of swirl number along the vortex tube.

The temperature of all adiabatic walls is assumed constant at 300 K. From the figure it can be observed that, the total temperature at the tube center for different positions along the hot tube length has a minimum value and it increases in the direction of tube wall.

The total temperature contours are presented in Fig. (10-b). From the figure, it can be noticed that the lowest temperature occurs at the core of the tube cross-section close to the entrance of the hot tube. The previous behavior due to the effect of change of swirl intensity on the temperature distribution along the hot tube.

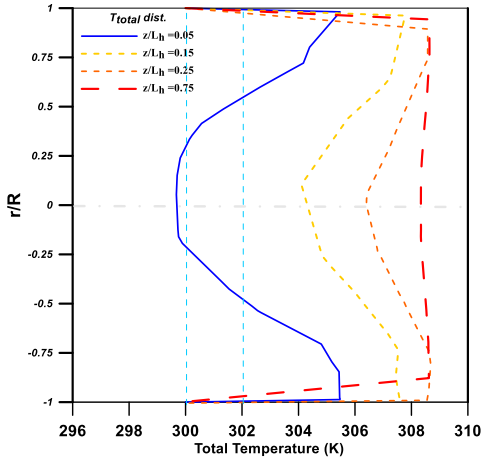

Fig.(10-a)

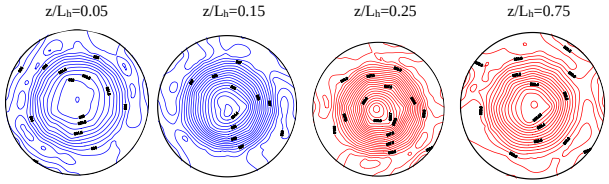

Fig.(10-b)

Figure (10): The temperature distribution along the hot tube.

4.2 Effect of geometrical parameters

In this section, the effect of some geometrical parameters on the temperature difference at the cold/hot outlets and coefficient of performance of vortex tubes are presented. These geometrical parameters are number of inlet nozzles, hot tube diameters and hot tube lengths.

4.2.1 Effect of numbers of inlet nozzles

Four geometries of vortex tube with different number of inlet nozzle (1, 2, 3 and 4) are created with constant inlet cross section area (i.e. inlet area of nozzle is divided on 2, 3 and 4 area). The effect of different number of inlet nozzles (1, 2, 3, and 4 nozzles) on the temperature difference is calculated of the suggested geometry with 25 cm hot tube length and 1 cm cold tube length. The inlet conditions are charged from 1 bar to 5 bar as total inlet pressure and constant total inlet temperature at 302 K. The inlet air mass flow rate is constant of all number of inlet nozzle at the same pressure. Figure (11) shows numbers of inlet nozzles effect on the cold and hot temperature at different total inlet pressure. From the figure, it is concluded that the maximum cold temperature difference is achieved when using two inlet nozzles which is consistent with [8], while the maximum hot temperature difference is occurring at one inlet nozzle for all values of inlet pressure.

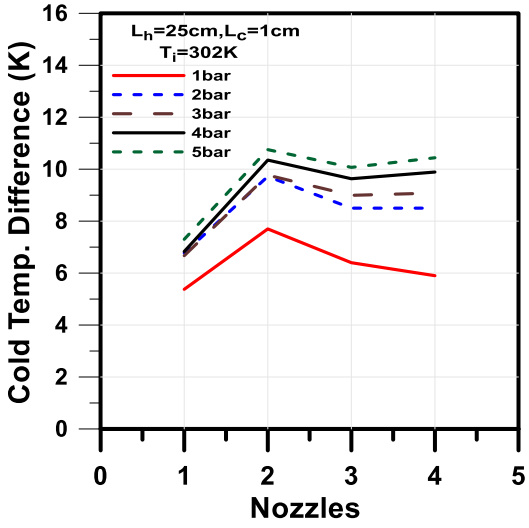

Fig.(11-a)

Figure (12-a) shows the effect of inlet nozzles number on the cooling coefficient of performance at different inlet pressure. From the figure, it can be observed that, the COP_c is decreased with increasing inlet pressure for all number of inlet nozzles as a result of increase of compression work. At the same time, using two inlet nozzles are achieved the maximum COP_c for all inlet pressure compared with other number of inlet nozzles. The reasons for low COP_c with the increase in inlet pressure, as a result of increase of compression work. At the same time the difference of cold temperature at $P\_i = 1bar$ considered somewhat large compared to the difference of hot temperature.

Figure (12-b) presents the effect of number of inlet nozzles on the heating coefficient of performance at different values of inlet pressure. It is observed that using one nozzle achieved the maximum COP_h at all inlet pressure. Additionally, the COP_h is decreased with increased inlet pressure.

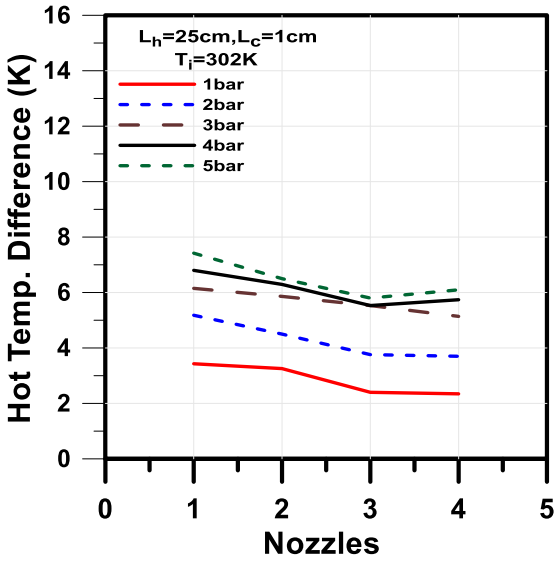

Fig.(11-b)

Figure (11): Effect of numbers of inlet nozzles on the temperature difference at different values of inlet pressure.

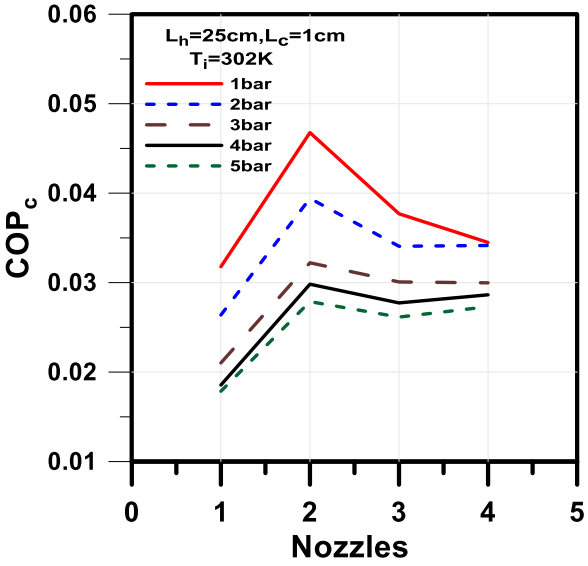

Fig. (12-a)

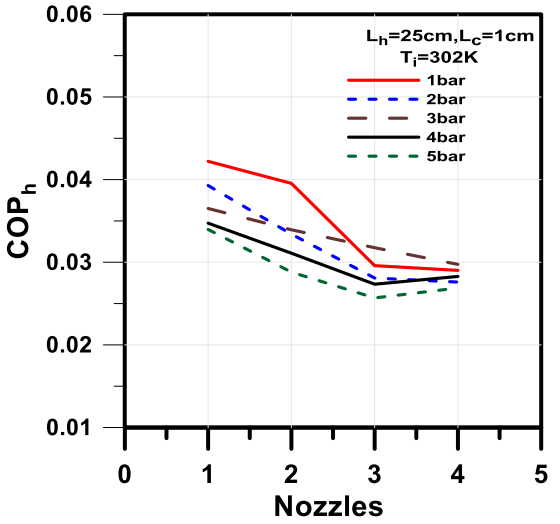

Fig. (12-b)

Figure (12): Effect of numbers of inlet nozzles on the coefficient of performance at different values of inlet pressure.

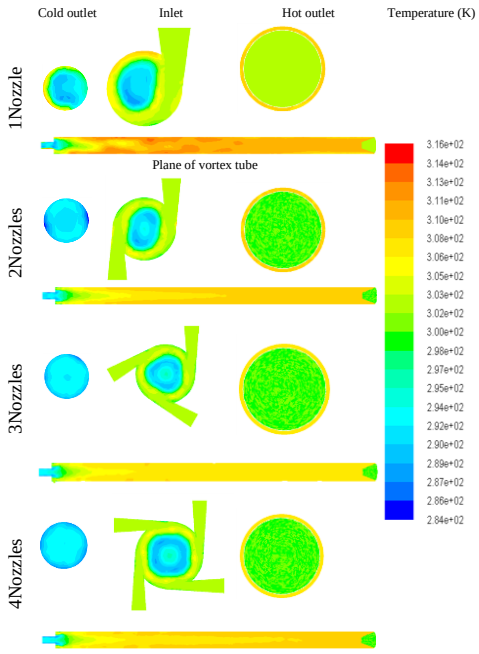

Figure (13): Contours of temperature for different number of inlet nozzles at constant inlet pressure 5 bar.

4.2.2 Effect of hot tube diameters

The effect of the different hot tube diameters (0.65 cm, 1.3 cm, and 1.95 cm) at constant diameter ratio ($D_c/D_h \approx 0.5$) on the temperature difference and vortex tube performance are discussed in this section. The results of the hot tube diameters effect are tested at L_h =25 cm, $L_c = 1\ cm$ and number of inlet nozzle, N =2. Figure (14) presents the effect of hot tube diameters on the cold and hot temperature difference at different values of inlet pressure. Figure (14-a) shows the variation of cold temperature difference with hot tube diameters and Fig. (14-b) depicts this effect on the hot temperature difference. From these figures, it can be noticed that the maximum temperature differences are achieved at ($D_h = 1.3\ cm$) approximately for both the cold and hot temperature difference at all inlet pressure values. But in cold temperature difference at higher inlet pressure the cold temperature difference is best at ($D_h = 1.95\ cm$).

Figure (13) depicts the filled contours of total temperature distribution at different number of inlet nozzles for inlet pressure equal to 5 bar. It can be observed that the total hot temperature region at the outlet of the hot tube is greater at one nozzle, and the region decreases with the increase the nozzles numbers. While the total cold temperature region at the outlet of the cold tube is greater in the presence of two inlet nozzles.

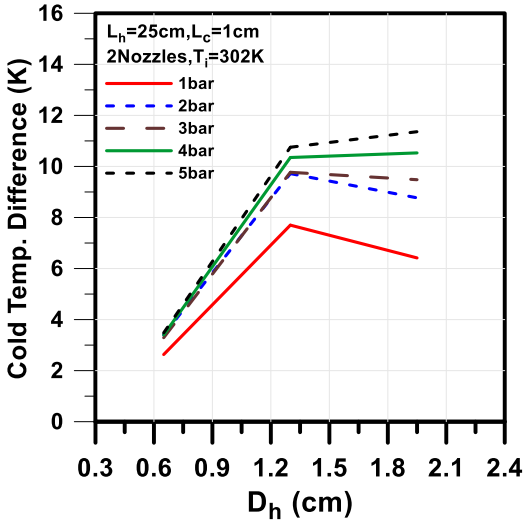

Fig. (14-a)

Figure (15) presents the effect of different hot tube diameters on the coefficient of performance at different values of inlet pressure. Figure (15-a) shows the variation of (COP_c) with different hot tube diameters and Fig. (15-b) depicts this effect on (COP_h). From these figures, it can be noticed that the maximum coefficient of performance is achieved at ($D_h = 1.3\ cm$) approximately for both (COP_c) and (COP_h) at all inlet pressure values.

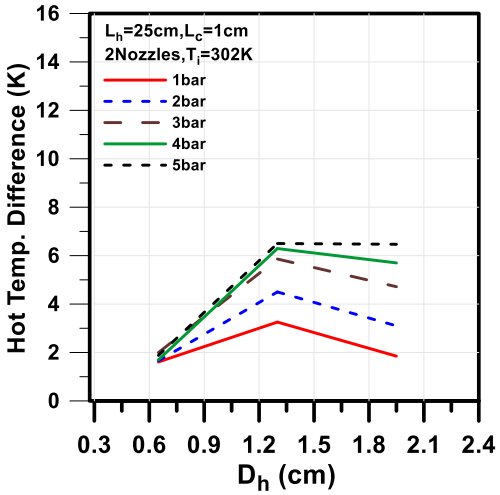

Fig. (14-b)

Figure (14): Effect of D_h on the cold and hot temperature difference at different inlet pressure.

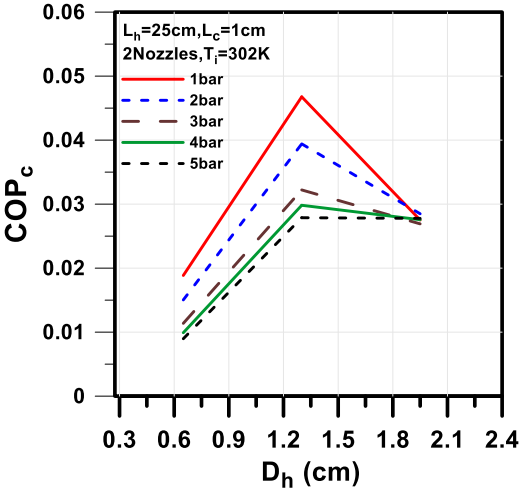

Fig. (15-a)

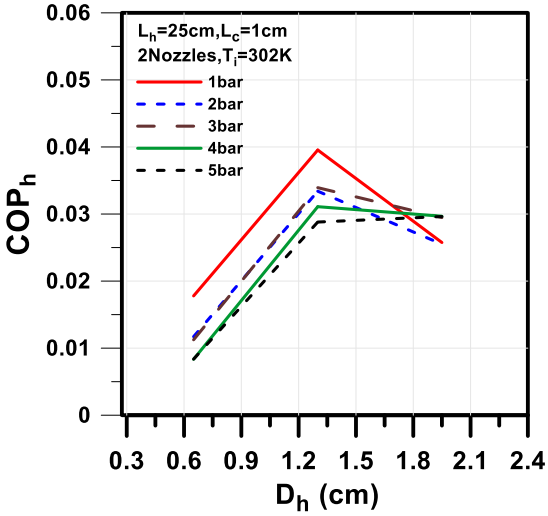

Fig. (15-b)

Figure (15): Effect of D_h on the cold and hot coefficient of performance at different inlet pressure.

4.2.3 Effect of hot tube lengths

The effect of hot tube lengths on the temperature difference of vortex tube and performance are studied. The different hot tube lengths are tested at (25 cm, 50 cm, and 75 cm). All results are carried out with a constant length of cold tube which is 1.0 cm. Figure (16) shows the variations of the cold temperature difference and hot temperature difference with different hot tube lengths at different inlet pressure. From the figures it can be cleared that the increase in the hot tube length tends to decrease in the cold and hot temperature difference at constant value of inlet pressure. The above behavior reflects the effect of hot tube length on the turbulence intensity and consequently on the energy separation through the vortex tube. Figure (17) presents the effect of different hot tube lengths on the coefficient of performance at different values of inlet pressure. Figure (17-a) shows the variation of (COP_c) with different hot tube lengths and Fig. (17-b) depicts this effect on (COP_h). From these figures, it can be noticed that the cold and hot coefficients of performance decreases with increasing the hot tube length and the inlet pressure.

4.3 Operating conditions

The effect of some operating conditions on cold/hot temperature difference of vortex tubes are investigated. These operation conditions are inlet pressure (P_i), and cold mass fractions ($\dot{m}_{cf}$).

4.3.1 Effect of inlet pressure

The effect of different values of inlet pressures on the hot and cold temperature difference in vortex tubes is shown in Fig. (18-a). Where Fig. (18-b) shows the same effect but on cooling and heating performance.

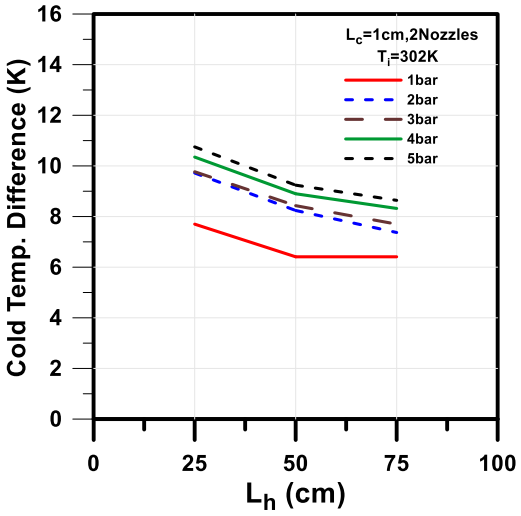

Fig. (16-a)

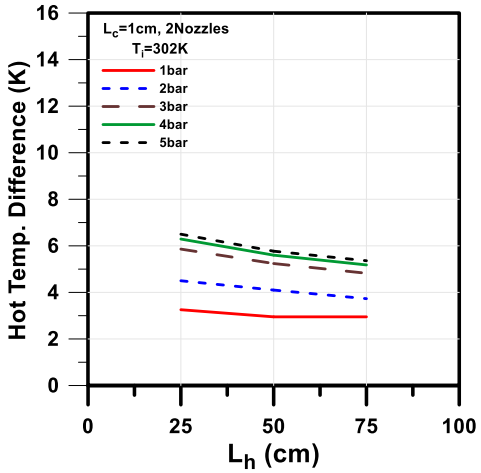

Fig. (16-b)

Figure (16): Effect of hot tube lengths on cold and hot temperature differences at different values of inlet pressure.

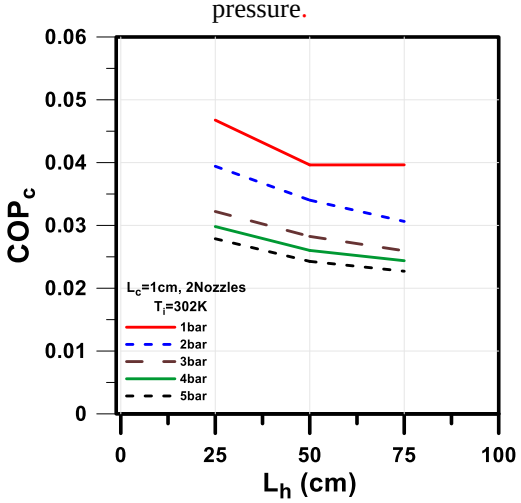

Fig. (17-a)

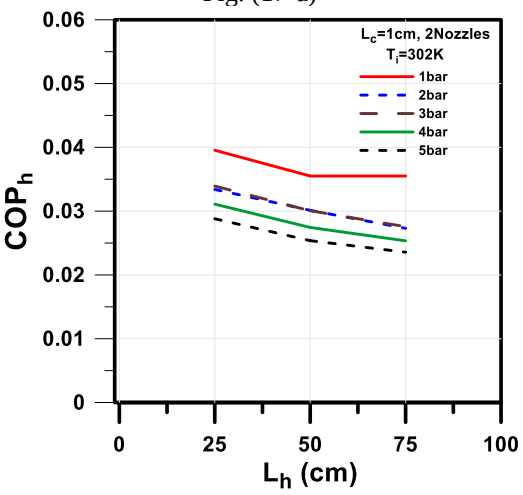

Fig. (17-b)

Figure (17): Effect of hot tube lengths on cold and hot coefficient of performance at different values of inlet pressure.

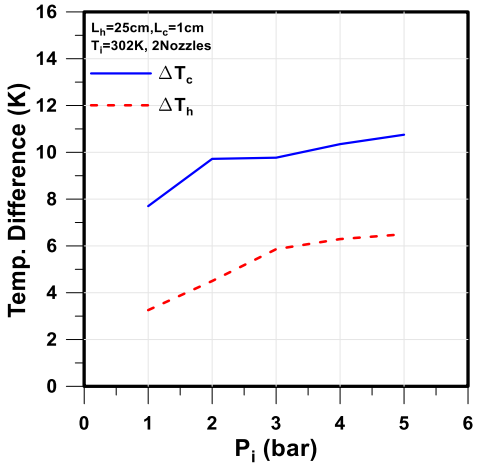

Fig. (18-a)

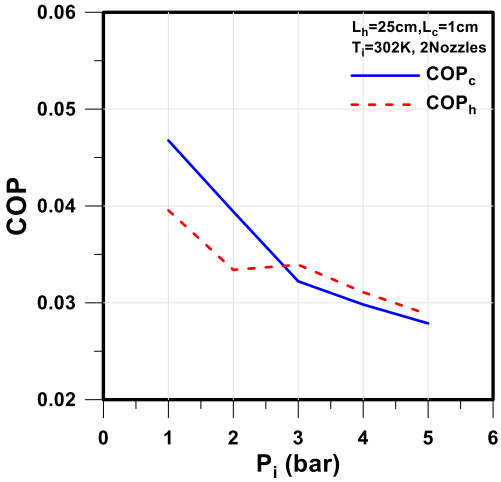

Fig. (18-b)

Figure (18): Effect of different values of inlet pressure on temperature difference and *COP*.

From Fig. (18-a), it can be noticed that the increase in inlet pressure increases the cold and hot temperature difference. The maximum temperature difference of cold $(T_i - T_c)$ is 11.2 K at $P_i = 5\,bar$. Also, the maximum difference of hot stream $(T_h - T_i)$ is 6.9 K approximately at $P\_i = 5\,bar$. From Fig. (18-b), it can be concluded that the increase in inlet pressure decreases the cooling and heating performance due to increase in compression work done. Therefore, the maximum (COP_c/COP_h) is achieved at small values of inlet pressure. Figure (19) presents the effect of inlet pressure on the cold mass fraction at different number of inlet nozzles. The results are obtained in conditions, $L_h = 25cm, L_c = 1\,cm, T_i = 302K$, and constant cone valve angle. From the figure, it can be concluded that the increase of inlet pressures at same number of inlet nozzle tends to increase in the cold mass fraction but the rate of increasing becomes very small at high value of inlet pressure. Also, from this figure it can be declared that, at constant value of inlet pressure, the cold mass fraction increases with increasing the

number of inlet nozzles, the value of increasing cold mass fraction is high when the number of inlet nozzle change from one to 2 nozzles and the value of increasing becomes small with more increasing number of inlet nozzles than 2.

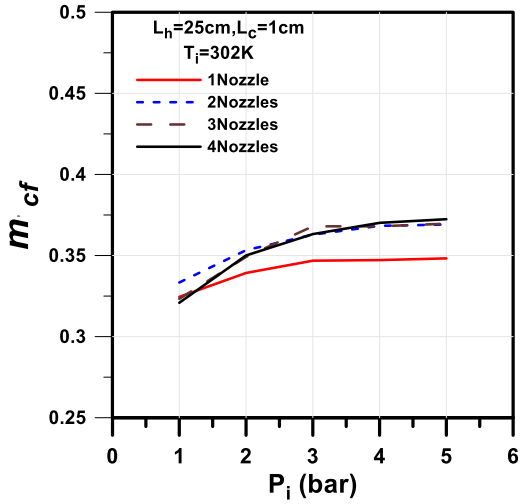

Figure (19): Effect of different values of inlet pressure on cold mass fraction at different number of inlet nozzles.

4.3.2 Effect of cold mass fraction

Cold mass fraction is one of the most important operating factors affecting vortex tube performance. Figure (20) presents the effect of cold mass fraction on the cold /hot temperature difference at different values of inlet pressure. From Fig. (20-a), it can be concluded that the cold temperature difference increases with increasing the cold mass fraction to reach the maximum value then decreases with more increasing of its value, The maximum cold temperature difference is achieved when the cold mass fraction change in the range $\dot{m}_{cf}$ ≈0.2 to $\dot{m}_{cf}$ ≈0.4 depends on the value of inlet pressure. At the same time, it can be noticed that from Fig. (20-b), the increase of cold mass fraction and inlet pressure increases the hot temperature difference. Figure (21) presents the effect of cold mass fraction on cold and hot coefficients of performance (COP_c/COP_h) at different values of inlet pressure. This figure indicates that the cold and hot coefficients of performance increase with increasing the cold mass fraction to reach the maximum value then decreases with more increasing of its value. The behavior of hot coefficient of performance reflects the effect of the rate of increasing the hot temperature difference at small values of cold mass fraction compared with that at high values of it. From Fig. (21-a), it can be concluded that, the maximum values of (COP_c) occurred approximately at $\dot{m}_{cf}$≈0.32 to $\dot{m}_{cf}$≈ 0.49 while, Fig. (21-b), showed the maximum values of (COP_h) achieved approximately at $\dot{m}_{cf}$≈0. 23 to $\dot{m}_{cf}$≈ 0.4.

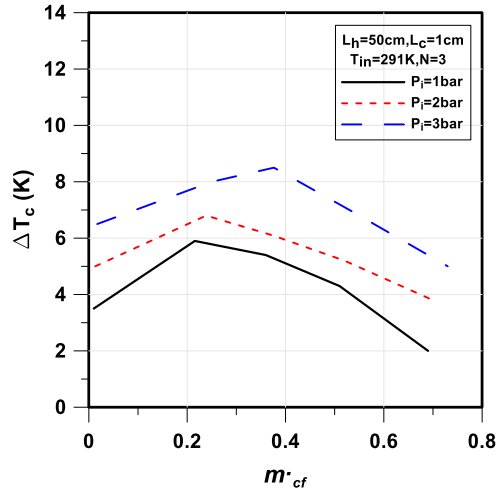

Fig. (20-a)

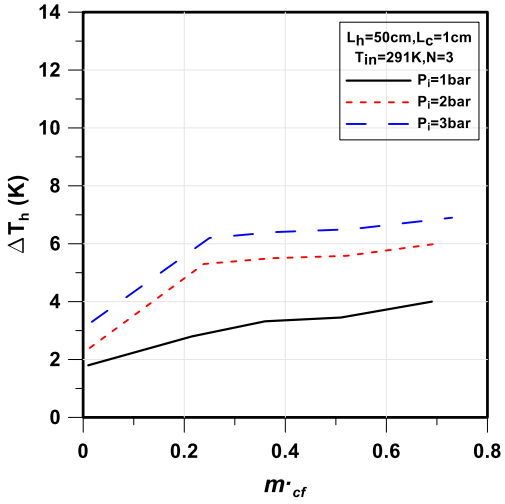

Fig. (20-b)

Figure (20): Effect of cold mass fraction on the cold /hot temperature difference at different values of inlet pressure.

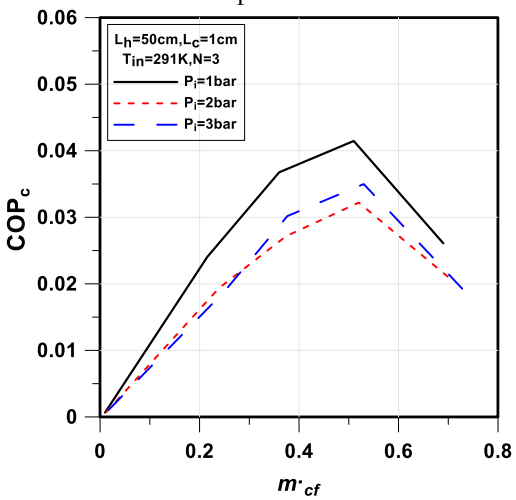

Fig. (21-a)

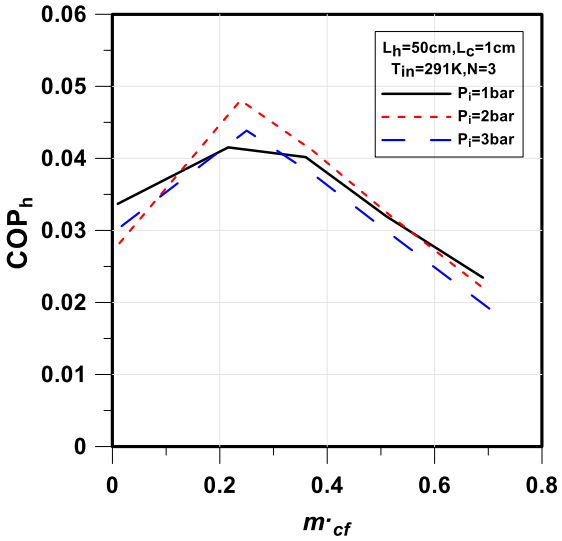

Fig. (21-b)

Figure (21): Effect of cold mass fraction on the cold and hot coefficient of performance at different values of inlet pressure

5. CONCLUSIONS

In the present study, CFD model is used to simulate the flow characteristics along the vortex tube. The theoretical model is validated with previous published data to determine the suitable turbulence model and test the model ability to predict the flow parameters vortex tube. Some operating conditions and geometrical parameters are tested to select the suitable conditions which achieve the best performance of the vortex tube. From the theoretical results, it can be concluded that:

1. The tangential velocity and swirl number are maximum at the position near the inlet nozzle and decrease on towards of hot exit. Also, the total temperature is maximum near the wall and minimum at core along the vortex tube.
2. The increase of inlet pressures causes increase in cold and hot temperature difference and decrease in the cooling and heating coefficient of performance.
3. The maximum cold temperature difference is achieved at a cold mass fraction $\dot{m}_{cf}$ from 0.22 to 0.36 based on inlet pressure while the hot temperature difference increased with increasing the cold mass fraction.
4. The hot tube diameter at $D_h = 1.3\,cm$ is achieved the maximum cold and hot temperature difference and heating and cooling performance of vortex tube.
5. The maximum difference of cold /hot temperature is occurring at $L_h = 25\,cm$. At the same time, the maximum heating and cooling performance of vortex tube is achieved at $L_h = 25\,cm$.
6. The maximum value of cold temperature difference and cold coefficient of performance occur when using two inlet nozzles, while the maximum value of hot temperature difference and hot coefficient of performance achieve at one inlet nozzle.

6. References

[1] S. Eiamsa-ard, K. Wongcharee, and P. Promvonge, "Experimental investigation on energy separation in a counter-flow Ranque-Hilsch vortex tube: Effect of cooling a hot tube," International Communications in Heat and Mass Transfer, vol. 37, no. 2, Feb. 2010., pp. 156–162

[2] T. Dutta, K. P. Sinhamahapatra, and S. S. Bandyopdhyay, "Comparison of different turbulence models in predicting the temperature separation in a Ranque-Hilsch vortex tube," International Journal of Refrigeration, vol. 33, no. 4, Jun. 2010, pp. 783–792.

[3] R. Shamsoddini and A. H. Nezhad, "Numerical analysis of the effects of nozzles number on the flow and power of cooling of a vortex tube," International Journal of Refrigeration, vol. 33, no. 4, Jun.2010, pp. 774–782.

[4] H. M. Skye, G. F. Nellis, and S. A. Klein, "Comparison of CFD analysis to empirical data in a commercial vortex tube," International Journal of Refrigeration, vol. 29, no. 1, Jan. 2006, pp. 71–80.

[5] R. Manimaran, "Computational analysis of flow features and energy separation in a counter-flow vortex tube based on number of inlets," Energy, vol. 123, 2017, pp. 564–578.

[6] Y. T. Wu, Y. Ding, Y. B. Ji, C. F. Ma, and M. C. Ge, "Modification and experimental research on vortex tube," International Journal of Refrigeration, vol. 30, no. 6, Sep. 2007, pp. 1042–1049.

[7] M. Attalla, H. Ahmed, M. Salem Ahmed, and A. Abo El- Wafa, "An experimental study of nozzle number on Ranque Hilsch counter-flow vortex tube," Experimental Thermal and Fluid Science, vol. 82, Apr. 2017, pp. 381–389.

[8] S. B. Bhote and K. D. Devade, "Investigations on Thermal Performance of Multi-Nozzle Ranque-Hilsch Vortex Tube," International Journal of Technology, vol. 8, no. 2, 2018, pp 65.

[9] I. Cebeci, V. Kirmaci, and U. Topcuoglu, "Les effets du nombre de tuyères à orifices et des tuyères faites de plastique en polyamide et

d'aluminium avec différentes pressions d'aspiration sur la performance de chauffage et de refroidissement des tubes vortex de Ranque-Hilsch à contre-courant: Une étude expérimentale," International Journal of Refrigeration, vol. 72, Dec. 2016, pp. 140–146.

[10] V. Kirmaci, H. Kaya, and I. Cebeci, "Analyse expérimentale et exergétique de la performance thermique d'un tube vortex de Ranque-Hilsch à contre- courant avec différents types de tuyères," International Journal of Refrigeration, vol. 85, Jan. 2018, pp. 240–254.

[11] P. Promvonge and S. Eiamsa-ard, "Investigation on the Vortex Thermal Separation in a Vortex Tube Refrigerator," ScienceAsia, vol. 31, no. 3, 2005, pp. 215–223.

[12] B. Markal, O. Aydin, and M. Avci, "An experimental study on the effect of the valve angle of counter-flow Ranque-Hilsch vortex tubes on thermal energy separation," Experimental Thermal and Fluid Science, vol. 34, no. 7, 2010, pp. 966–971.

[13] K. Dincer, S. Baskaya, B. Z. Uysal, and I. Ucgul, "Experimental investigation of the performance of a Ranque-Hilsch vortex tube with regard to a plug located at the hot outlet," International Journal of Refrigeration, vol. 32, no. 1, Jan. 2009, pp. 87–94.

[14] A. T. Pise and K. D. Devade, "Investigation of Refrigeration Effect Using Short Divergent Vortex Tube," International Journal of Earth Sciences and Engineering, vol. 5, no. 1, 2012, pp. 278–284.

[15] J. Prabakaran and S. Vaidyanathan, "Effect of diameter of orifice and nozzle performance of counter flow vortex tube," International Journal of Engineering Science and Technology, vol. 2, no. 4, 2010, pp.704-707.

[16] J. Prabakaran and S. Vaidyanathan, "Effect of orifice and pressure of counter flow vortex tube," Indian Journal of Science and Technology, vol. 3, no. 4, 2010, pp. 705-714.

[17] M. O. Hamdan, S. A. B. Al-Omari, and A. S. Oweimer, "Experimental study of vortex tube energy separation under different tube design," Experimental Thermal and Fluid Science, vol. 91, Feb. 2018, pp. 306–311.

[18] M.H. Saidi, M.S. Valipour "Experimental modeling of vortex tube refrigerator", Applied Thermal Engineering 23, 2003, pp.1971–1980.

[19] James Cartlidge, Nafiz Chowdhury, Thomas povey "Performance characteristics of a divergent vortex tube'' International Journal of Heat and Mass Transfer, Vol. 186, May 2022.

[20] Ahmad M.Alsaghir, Mohammad O.Hamdana, Mehmet F.Orhan,MahmoudAwadb "Numerical and sensitivity analyses of various design parameters to maximize performance of a Vortex Tube" International Journal of Thermofluids,vol.13, 2022.

[21] Xingwei Liu, Zhongliang Liu "Investigation of the energy separation effect and flow mechanism inside a vortex tube", Applied Thermal Engineering, Vol. 67, 2014, pp.494–506.

[22] Qijun Xu, Jing Xie "Numerical simulation of the effect of different numbers of inlet nozzles on vortex tube" Process, vol.9, 2021, pp. 15-31.

[23] Hüseyin Kayaa, Onuralp Uluerb, Evren Kocaoğluc,Volkan Kirmacia "Experimental analysis of cooling and heating performance of serial and parallel connected counter-flow Ranquee–Hilsch vortex tube systems using carbon dioxide as a working fluid," International Journal of Refrigeration,Vol.106, 2019, pp.297-307.

[24] C.Biegger, C. Sotgiu, B.Weigand "Numerical investigation of flow and heat transfer in a swirl tube ", International Journal of Thermal Sciences,Vol. 96, 2015 pp.319–330.

Nomenclature

$c_{\varepsilon 1}, c_{\varepsilon 2}, c_{\varepsilon 3}$ Constants of turbulence models [-]
C Velocity [m/s]
C_p Specific heat at constant pressure [J/Kg. K]
D Diameter of vortex tube[m]
E Total energy [J]
G_b Generation of turbulence kinetic energy due to buoyancy $[m^2/s^2]$
G_k Generation of turbulence kinetic energy $[m^2/s^2]$
G_ε Generation of turbulence dissipation rate
g Acceleration gravity $[m/s^2]$
K Turbulence kinetic energy $[m^2/s^2]$
K_{eff} Effective thermal conductivity [w/m. K]
L Length of vortex tube [m]
$\dot{m}$ Mass flow rate [kg/s]
N Number of nozzles
P Pressure [bar]
Pr_t Turbulent Prandtl number
S Swirl number
S_k, S_ε Component of deformation rate
R Correlation coefficient
T Temperature [K]
Y_m Contribution of the fluctuating dilatation
Δ The difference [-]
γ Specific heat ratio [–]

ε Turbulence dissipation rate $[m^2/s^3]$
μ Dynamic viscosity $[kg/m.s]$
ρ Density $[Kg/m^3]$
τ_{ij} Stress tensor component$[N/m^2]$
ν Kinematic viscosity $[m^2/s]$

Subscripts

a atmosphere
c cold
cf cold fraction
h hot
i, in inlet

Abbreviations

COP Coefficient of performance
CFD Computational fluid dynamic
RNG Renormalization group
RHVT Ranque-Hilsch vortex tube